Tunable Metasurfaces for Filtering the Electromagnetic Waves Under Different Excitations

Sultan Can[1], Emrullah Karakaya [2], Fulya Bagci[2], Asim E. Yilmaz[1], and Baris Akaoglu[2]

[1] Department of Electrical and Electronics Engineering
Ankara University, Ankara, 06830, Turkey
sultancan@ankara.edu.tr, aeyilmaz@eng.ankara.edu.tr

[2] Department of Engineering Physics
Ankara University, Ankara, 06100, Turkey
emrullah.fizik@gmail.com, fbagci@eng.ankara.edu.tr, akaoglu@eng.ankara.edu.tr

Abstract ─ In this study a tunable metasurface has been presented and evaluated for different excitation types. Tunability has been achieved by changing the substrate and geometrical properties. In order to obtain uniqueness, a parameter retrieval for the effective permittivity and permeability is performed using a version of the Nicholson-Ross-Weir (NRW) algorithm that is improved by implementing the Kramers-Kronig relationship. The results regarding the parametric and retrieval analysis are presented.

Index Terms ─ Double negative materials, electronic band gap, ε-negative materials, frequency selective surfaces, metamaterials, single negative materials.

I. INTRODUCTION

Electronic devices, which incredibly penetrate our daily life, make the electromagnetic pollution problem more critical and the researchers pay significant attention in order to cope with those problems. The protection of electromagnetic waves are necessary not only in terms of human health but also to prevent the devices to interact with each other. Several methods are used for shielding including designing frequency selective surfaces (FSS), left handed materials, double negative materials (DNG), single negative materials (SNG), plasmons, electronic band gap structures (EBG) and artificial magnetic conductors (AMC).

Metamaterials are artificial materials, which can satisfy having simultaneously negative values of permeability (μ) and permittivity (ε). The theory of the metamaterials goes back to 1968 in which Veselago claimed that such materials have extra-ordinary properties unlike the ordinary right-handed materials [1]. Metamaterials are referred to as left-handed materials and can have double or single negative values of permittivity and permeability. Those materials can achieve reverse Doppler Effect, reverse Vavilov-Cerenkov effect and negative index of refraction. The realization of metamaterials is first handled by Pendry *et al.* by achieving ε-negative values by using the thin-wire array structures, based on the plasma theory [2-4]. Although the realization of the ε-negative materials could be accomplished since, free electric charges exist in nature, the μ-negative materials were still a problem due to the absence of magnetic charges. This handicap is overcome by the invention of the split-ring resonators (SRRs). Smith and his group realized μ-negative materials by exciting the SRRs magnetically and afterwards Shelby experimentally showed that double negative materials could be achieved by combining conductor rods and SRRs [5,6]. Some modifications are introduced thereafter in SRRs and SRR-type structures such as edge- and broadside-coupled SRRs, complementary SRRs (CSRRs) or spiral resonators are developed [7-9]. Electric-*LC* (ELC) resonators are later proposed, offering more practicality in realization [10].

Engineered-surfaces are required for filtering the electromagnetic waves and having single or double negative properties. The most familiar example of the μ-negative material can be regarded as the SRR structure. A band of frequencies where the effective permeability is negative is shown to cause attenuation of scattering for the 3D arrangement of SRR arrays when illuminated by an incident electromagnetic wave with a magnetic field vector axial to the rings [4]. Similarly, the negative image structure of the SRR, so-called the complementary SRR is demonstrated to exhibit an ε-negative behavior [8]. Another approach to obtain an ε-negative metamaterial is to use ELC resonator [10]. These resonators can be combined with microstrip technology and compact stop band filters can be designed, thanks to the sharp change of ε from positive to negative in the vicinity of resonance [8,9]. ε-negative and μ-negative materials can also find applications in the design of miniaturized antennas [11-14]. A miniaturized dual band antenna is designed by

Submitted On: September 29, 2015
Accepted On: June 17, 2016

embedding an ε-negative and a DNG inclusion in a single dipole antenna [12]. By combining the double negative property with conventional right-handedness, compact metamaterial antennas with omni-directional radiation patterns are demonstrated [13,14]. Continuous scanning of radiation angle can be realized in these antennas by loading the structure with varactors and tuning the bias voltage [14]. SNG materials can also be used in the reduction of the specific absorption rate values of portable electronic devices, such as cell phones and for this purpose there are several studies conducted in the literature [15,16].

In this study, a window-like shaped novel metasurface structure is proposed and evaluated in terms of permittivity and permeability for both electrical and magnetic excitation types. The proposed structure is a promising metasurface, which can be modified easily to be as either a single band or dual band filter by opening or closing the aperture on the conductor part of the FSS. It also satisfies the tunability feature.

In addition to tuning of aperture length, the frequency tunability can also be achieved by changing the FSS copper strip width or substrate properties. It is noteworthy to mention that these changes do not affect the attenuation of the filter while tuning the operation frequency. The proposed structure with gap has double band characteristics for C-band and K_u-band. C-band can be used for applications such as satellite transponders and K_u-band for application areas such as high-resolution imaging and for satellite transponders.

An improved algorithm for extracting the effective constitutive parameters of a metamaterial is proposed by Szabo *et al.* [17] and achieved satisfactory results for the sparse unit cell models with the proper periodicity. The procedure presented in the mentioned paper invokes the Kramers–Kronig relations to ensure the uniqueness of the solution. The accuracy of the mentioned method is demonstrated by retrieving the effective material parameters of a homogeneous slab [17].

Due to the approved accuracy, we used the corresponding algorithm for retrieving the permittivity and permeability values. The results obtained from the algorithm are presented in the following sections as well as the parametric analysis results of the proposed structure. Impact of substrate thickness, permittivity, copper strip width, gap length, and excitation types are evaluated regarding the parametric analysis.

II. PROPOSED FSS GEOMETRY AND BOUNDARY CONDITIONS

The proposed geometry is presented in Fig. 1 where the parameter g is assumed zero at the beginning of the design, which corresponds to the case of "no gap" in the structure. The substrate thickness and the conductor thickness are denoted by h and h_c, respectively. The conductor part is etched to the dielectric layer. As it is seen on the Fig. 1 (a), c denotes the gap between the edge and the conductor, x denotes the width of the side gratings, and also the width of the mid-strips are equal to x.

The scattering parameters are calculated and the electric field, magnetic field and surface current properties of the structure under resonance are evaluated using the CST Microwave Studio full-wave software with unit cell boundary conditions. Besides a detailed parametric analysis, the impacts of different types of excitations are investigated in this study. For this reason, the proposed structure is excited by a plane wave perpendicular to the FSS plane with its E-field along the gap for the analyses in Section III (Fig. 1 (b)). For the analyses in Section IV, the structure is excited from one side with an H-field perpendicular to the FSS plane (Fig. 1 (c)).

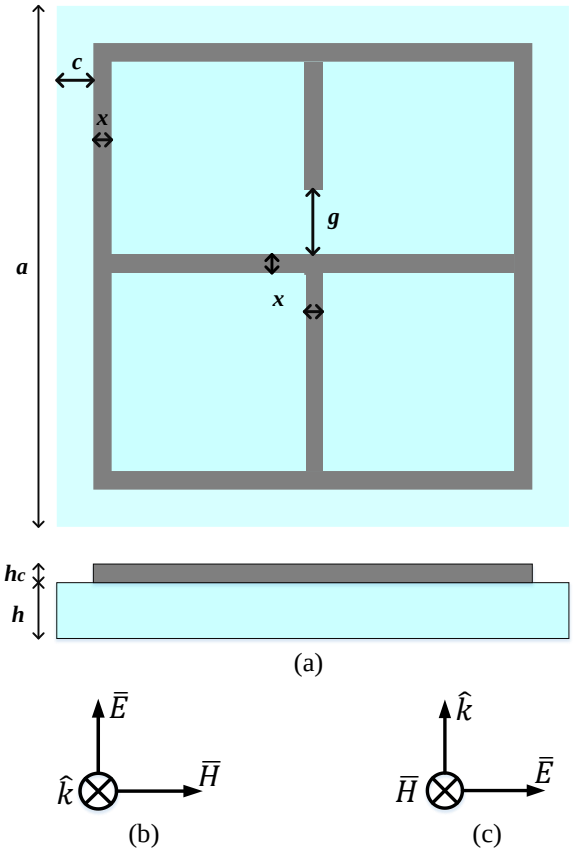

Fig. 1. (a) Geometry of the proposed FSS structure, (b) electric excitation, and (c) magnetic excitation.

III. ELECTRICALLY EXCITED FSS GEOMETRY

A. Impact of substrate thickness

Thickness of the substrate has a significant effect on scattering parameters and bandwidth. The resonance characteristics of S_{11} parameter is affected from the

change of the thickness of the substrate. Resonance frequency of the S_{11} is 12.8 GHz for a thickness value of 0.2 mm and reduces to 12.24 GHz for a thickness value of 0.4 mm. S_{11} resonance occurs at 11.7 GHz, 11.6 GHz and 11.52 GHz for thickness values of 0.6 mm, 0.8 mm and 1 mm, respectively. The change of the value of the resonance frequency is in a much less amount for thicker substrates. S_{11} bandwidth, which is considered as the 10 dB bandwidth, also reduces from 2.67 GHz to 2.19 GHz for the thickness values 0.2 mm to 1 mm. The results regarding the thickness effect to S_{11} parameter is presented in Fig. 2 (a) and that to S_{21} parameter is demonstrated in Fig. 2 (b).

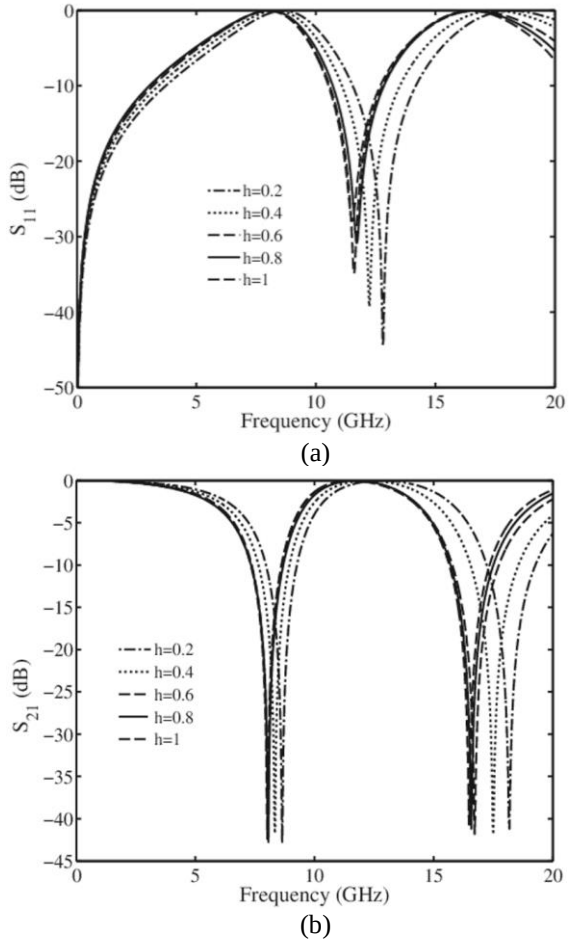

Fig. 2. Impact of substrate thickness to: (a) S_{11} and (b) S_{21} parameter. a=10 mm, x=0.1 mm, g=1 mm, c=1 mm, h=1 mm, h_c=0.035 mm, ε_r=2.2.

As seen in Fig. 2 (b) dual resonance is observed for S_{21} parameter. Lower S_{21} resonance frequency is decreased from 8.64 to 8.02 GHz with the increment of the thickness value from 0.2 mm to 1 mm. As a similar characteristic, the higher S_{21} resonance frequency is decreased from 18.18 GHz to 16.4 GHz for the aforementioned thickness values. S_{21} bandwidth is varied between 1.28 GHz to 1.39 GHz for the lower frequency and 2.74 to 1.71 GHz for the higher frequency. As expected, the thicker substrates caused wider band values.

B. Impact of substrate permittivity

In order to evaluate the impact of the substrate properties, Rogers RT5880, Arlon350and FR4 are considered as substrates of the proposed structure since they are the most used substrates in most of the applications including periodic structures and antennas, having a permittivity value of ε_r=2.2, ε_r=3.5 and ε_r=4.3, respectively. The corresponding results are demonstrated in Fig. 3.

S_{11} characteristics of the proposed structure with respect to the varied parameter, the permittivity, is demonstrated in Fig. 3 (a) and the S_{21} parameter is shown in Fig. 3 (b). As shown in Fig. 3 (a), the S_{11} resonances are at 11.5 GHz, 9.58 GHz and 8.74 GHz for the permittivity values of 2.2, 3.5 and 4.3, respectively.

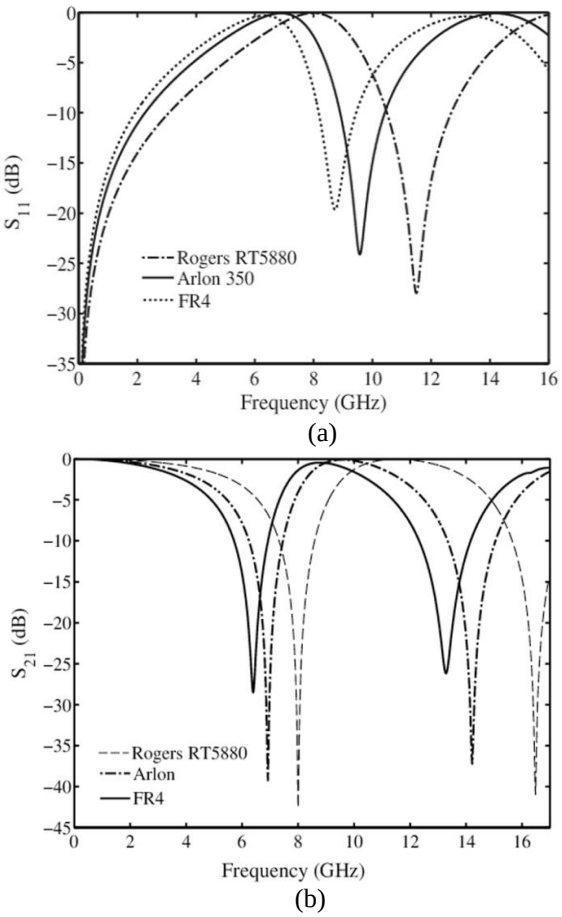

Fig. 3. Effect of substrate to: (a) S_{11} and (b) S_{21}. a=10 mm, x=0.1 mm, g=1 mm, c=1 mm, h=1 mm, h_c=0.035 mm, ε_r=2.2 (Rogers RT5880), ε_r=4.3 (FR4), ε_r=3.5 (Arlon350).

The higher permittivity values caused lower resonance values, as expected. The bandwidth values are observed as 2.22 GHz, 1.51 GHz and 1.3 GHz for the increasing value of permittivity. S_{21} resonance values are observed at 8 GHz, 6.92 GHz and 6.4 GHz for the lower frequency band and at 16.48 GHz, 14.22 GHz and 13.28 GHz for the upper resonance frequencies, for the permittivity values of 2.2, 3.5 and 4.3, respectively. The change in bandwidth values for the lower S_{21} resonance was negligible and around 1.22GHz and around 1.7 GHz for the lower and upper resonance bands, respectively.

C. Impact of copper strip width (*x*)

Impact of the copper strip width is also worth to evaluate since it directly affects the mutual impedance and changes the resonance frequency and bandwidth. For that purpose, the copper width *x* is varied between 0.1 mm to 0.5 mm and the effects of the parameter to S_{11} and S_{21} are presented in Figs. 4 (a) and 4 (b), respectively.

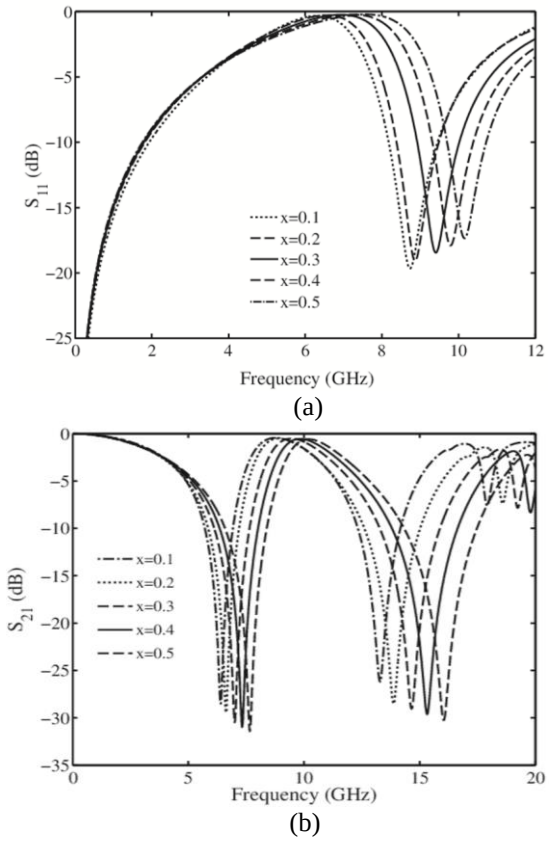

Fig. 4. Effect of *x* size to: (a) S_{11} and (b) S_{21}. a=10 mm, x=0.1 mm, g=1 mm, c=1 mm, h=1 mm, h_c=0.035 mm, ε_r=2.2.

S_{11} resonance frequencies are found to be 8.73 GHz, 8.86 GHz, 9.42 GHz, 9.79 GHz and 10.157 GHz for *x* values of 0.1, 0.2, 0.3, 0.4 and 0.5 mm, respectively. The increment of the copper width causes an increment in resonance frequency; however, it causes a decrement in bandwidth. The bandwidth is decreased from 1.28 GHz to 1.002 GHz when the copper width is increased to 0.5 from 0.1 mm. As the *x* increases, the inductance decreases and therefore the decrement of the resonance frequency confirms our expectations.

S_{21} resonances for the aforementioned copper thicknesses are observed as 6.4 GHz, 6.62 GHz, 7 GHz, 7.32 GHz and 7.66 GHz for lower band frequencies with a bandwidth value of 1.19 GHz, 1.37 GHz, 1.5 GHz, 1.65 GHz and 1.8 GHz respectively. The upper band S_{21} resonances occur at 13.28 GHz, 13.88 GHz, 14.64 GHz, 15.32 GHz and 16.04 GHz with a bandwidth value of 1.84 GHz, 2.43 GHz, 2.59 GHz, 2.85 GHz and 3.159 GHz, respectively.

D. Impact of gap length (*g*)

The proposed structure has an aperture on the conductor part of the FSS from the center and this gap has a significant effect on resonance frequencies. Inserting this gap automatically increases the number of resonances when compared with the structure without gap. The impact of the gap is also evaluated and the results are presented in Fig. 5.

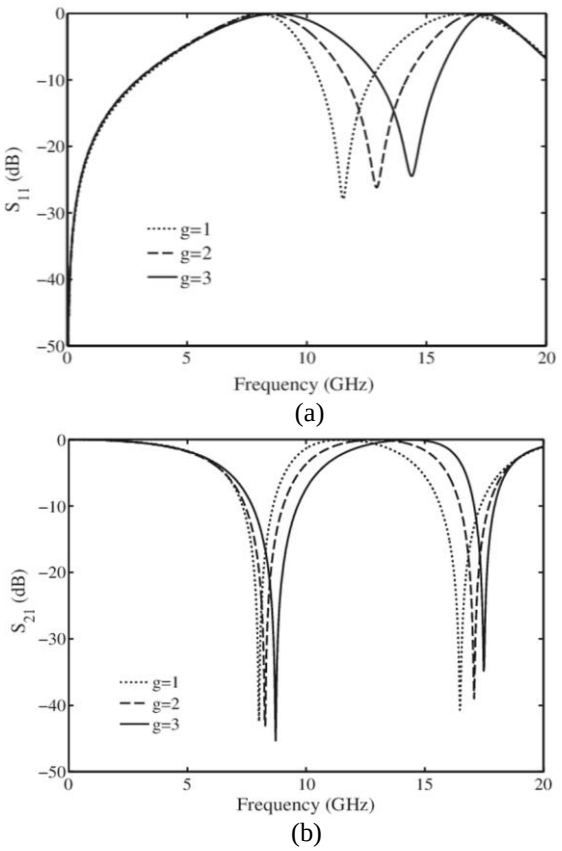

Fig. 5. Effect of gap width to: (a) S_{11} and (b) S_{21}. a=10 mm, x=0.1 mm, g=1 mm, c=1 mm, h=1 mm, h_c=0.035 mm, ε_r=2.2.

S_{11} resonance values increase to 14.98 GHz from 11.52 GHz with the increment of the gap from 1 mm to 3 mm. The increase of the resonance frequency can be explained with the decrease of the capacitance by the increase of the gap length. Bandwidth for the gap values 1 mm, 2 mm and 3 mm are 2.17 GHz, 2.49 GHz and 2.44 GHz, respectively.

Tunability is obtained not only in resonance values of S_{21} but also in bandwidth values of S_{21} for both upper (at K_u band around 16 GHz) and lower frequency bands (at X-band, around 8 GHz). Bandwidth of the S_{21} lower resonance frequency band is increased to 1.89 GHz from 1.28 GHz and the bandwidth of the S_{21} upper resonance frequency band is reduced to 0.89 GHz from 1.73 GHz.

E. Parameter retrieval results of electrically excited FSS geometry for "with" and "without gap"

The structures with and without gap are considered and the retrieval algorithm is applied in order to obtain the permittivity and permeability values.

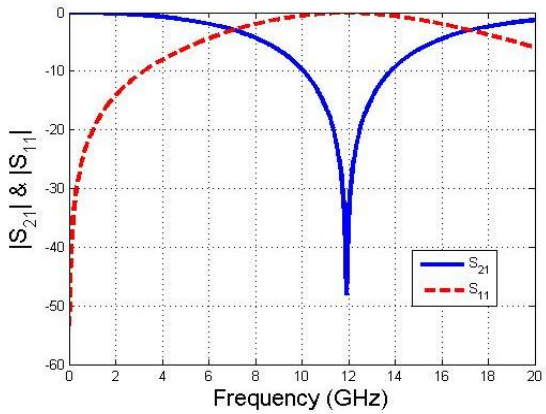

Fig. 6. Scattering parameters of a structure without gap (a=10 mm, x=0.1 mm, g=0 mm, c=1 mm, h=1 mm, h_c=0.035 mm, Rogers RT 5880).

The structure without gap has a single S_{21} resonance as expected due to the surface current distribution and the scattering characteristics are presented in Fig. 6.

Permittivity and permeability values are retrieved by using the magnitude and the phase information of the structure over a particular period and the results are presented in Fig. 7. As seen in the Fig. 7 (a), permittivity has negative values between 10.8 GHz and 17 GHz with a center frequency at 12 GHz. Since the structure is electrically excited, it was expected to have a negative permittivity value over a frequency region around resonance, but not a negative value of permeability value over the band of evaluation. The results presented in Fig. 7 (b) approves this expectation. The real permeability value is observed positive for the entire band.

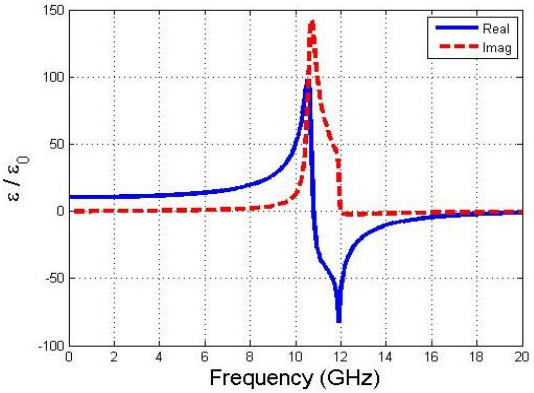

(a)

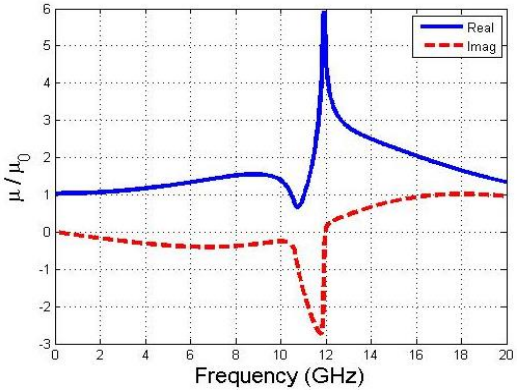

(b)

Fig. 7. Retrieved permittivity and permeability values (a=10 mm, x=0.1 mm, g=0 mm, c=1 mm, h=1 mm, h_c=0.035 mm, Rogers RT 5880).

The algorithm confirms well the expected negative permittivity behavior around the resonance frequency of the gap (see Fig. 6), although there exists a small inconsistency of the algorithm which accounts for the negative imaginary permeability in a narrow frequency region.

As aforementioned, the gap value (g) is one of the important parameters, which changes the surface currents and even increasing the number of the resonances of the structure. For that purpose, a gap having 1mm length is inserted to the structure and the structure is excited with a plane wave, which has an electrical field vector in parallel to this gap. The resulting scattering parameters are presented in Fig. 8.

As shown in Fig. 8 the structure has two S_{21} resonances, lower resonance is at 8.02 GHz and the upper resonance is at 16.5 GHz. The S_{11} resonance is occurred at 11.5 GHz with a bandwidth of 2.14 GHz.

The results regarding the permittivity and permeability retrieval are presented in Figs. 9 (a) and (b). The permittivity is negative around the resonance frequencies of 8.02 GHz and 16.5 GHz. When compared

with the "no-gap" case, the opening of the gap creates two negative-permittivity regions in the [0, 20 GHz] frequency interval. This can be explained by the occurrence of an additional resonance for the "with gap" structure.

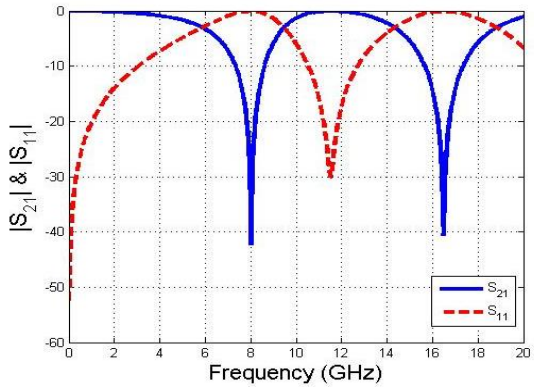

Fig. 8. Scattering parameters of the structure with gap for which the parametric retrieval algorithm is conducted (a=10 mm, x=0.1 mm, g=1 mm, c=1 mm, h=1 mm, h_c=0.035 mm, Rogers RT 5880).

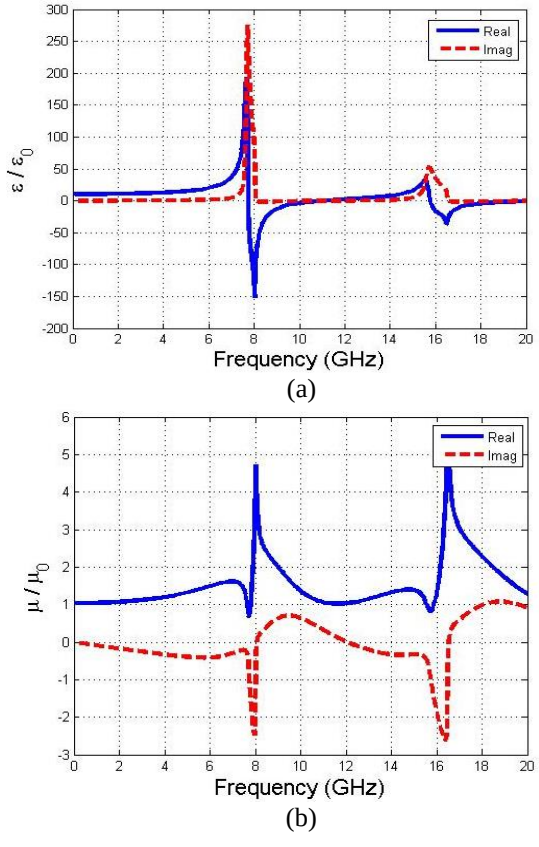

Fig. 9. (a) Retrieved permittivity and (b) permeability values of the structure with gap (a=10 mm, x=0.1 mm, g=1 mm, c=1 mm, h=1 mm, h_c=0.035 mm, Rogers RT 5880).

IV. MAGNETICALLY EXCITED FSS

Excitation type is another parameter that affects the resonance characteristics of the structure. Around resonance, a structure may show single or double negative properties when excited electrically, or magnetically. The magnetic excitation causes surface currents on the conductor part of the structure and resonance can occur due to this surface current. In order to show the difference between electric and magnetic excitation types for the proposed structure, several simulations are performed including the impact of the substrate thickness, substrate permittivity, gap length, copper strip width and the results are demonstrated.

A. Impact of substrate thickness

Impact of substrate thickness is evaluated and the scattering parameter results are presented in Fig. 10. The thickness values are varied between 0.2 mm to 1 mm and a resonance has been obtained in the S_{11} parameter. However, no resonance is occurred for S_{21}. Unlike the electric excitation case, changing the thickness value exhibits a negligible effect on the scattering characteristics of the magnetically excited structure.

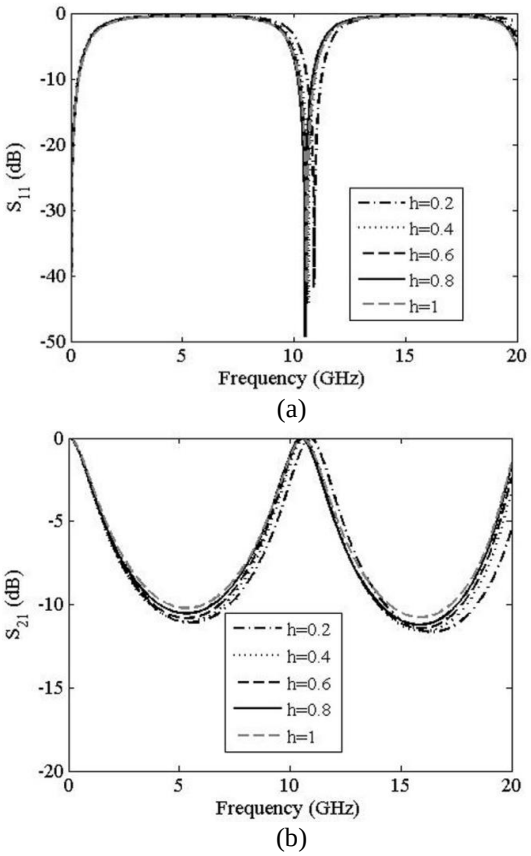

Fig. 10 Effect of substrate thickness of a magnetically excited structure to: (a) S_{11} and (b) S_{21} (a=10 mm, x=0.1 mm, g=1 mm, c=1 mm, h=1 mm, h_c=0.035 mm, ε_r=2.2).

B. Impact of substrate permittivity

The effect of using different substrates is also evaluated by considering FR4 (ε_r=4.3), Arlon350 (ε_r=3.5) and Rogers RT5880 (ε_r=2.2) as substrate materials. Similar to the electrically excited metasurface structure, as the permittivity of the substrate decreases, the resonance bands shift to higher frequencies, as shown in Fig. 11.

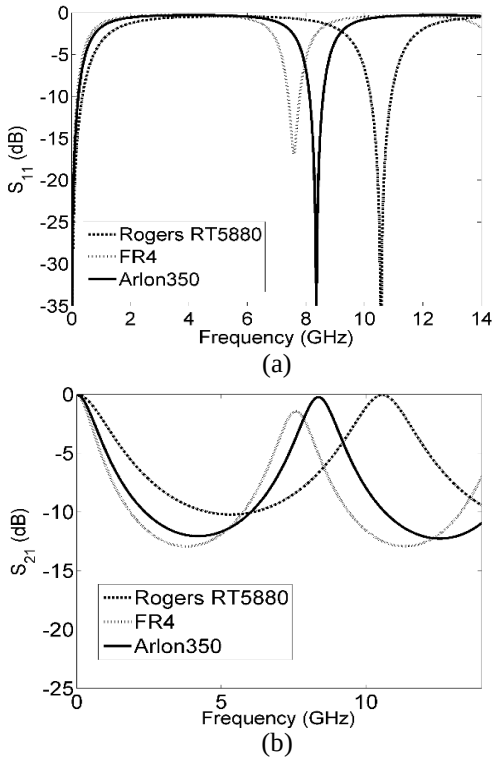

Fig. 11. Effect of substrate to: (a) S_{11} and (b) S_{21}. (a=10 mm, x=0.1 mm, g=1 mm, c=1 mm, h=1 mm, h_c=0.035 mm, ε_r=2.2 (Rogers RT5880), ε_r=4.3 (FR4), ε_r=3.5 (Arlon350)).

C. Impact of the copper strip width (x)

Similar to the thickness effect, the width of the copper strip does not affect the scattering characteristics as shown in Fig. 12 (a) for S_{11} and Fig. 12 (b) for S_{21}.

The magnetic field and surface current distribution of the structure are investigated at the resonance frequency of 10.56 GHz in order to clarify the underlying physics for the invariance of the resonance frequency against x change.

The magnetic field and surface current distribution are shown in Figs. 13 (a) and (b), respectively for the structure with g=1 mm, x=1 mm and ε_r=2.2. Magnetic field strength is primarily distributed in the outer sides of the outer metal strips and most of the current circulates on the outer side of the metal strip and in opposite directions for adjacent cells, as can be seen in Figs. 13 (a) and (b), respectively. Therefore the change of the metal strip width, x, does not affect the resonance characteristics, even for thicker strip values.

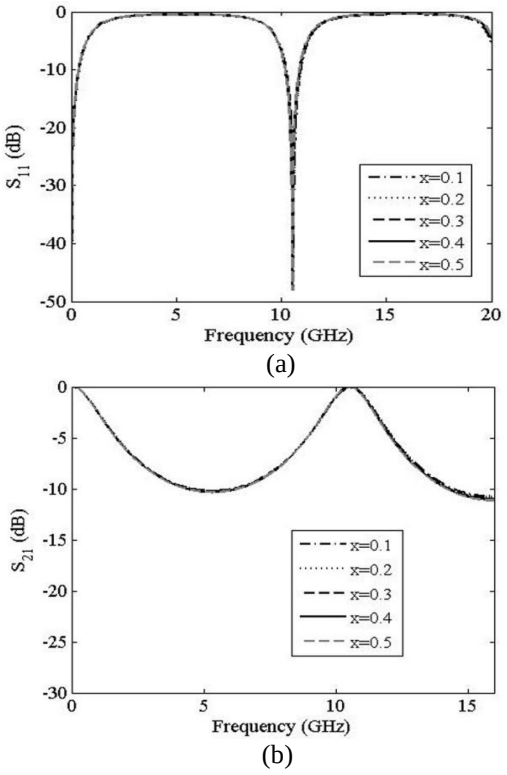

Fig. 12. Effect of copper width of a magnetically excited structure to: (a) S_{11} and (b) S_{21} (a=10 mm, g=1 mm, c= 1 mm, h=1 mm, h_c=0.035 mm, ε_r=2.2).

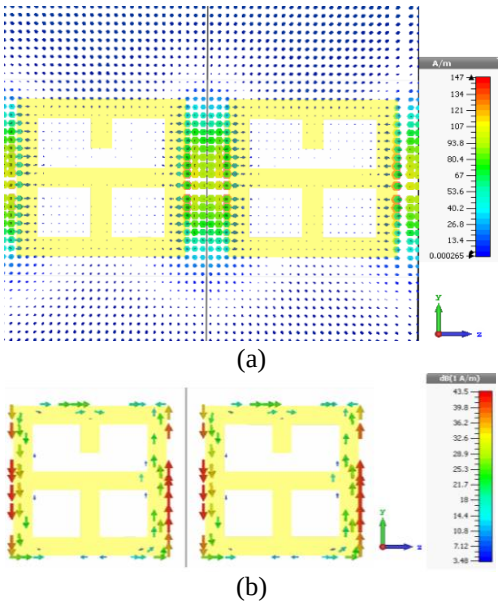

Fig. 13. (a) Magnetic field distribution and (b) surface current distribution of the structure with a=10 mm, x=1 mm, g=1 mm, c=1 mm, h=1 mm, h_c=0.035 mm, and ε_r=2.2, is shown in yz-plane. Since the structure is periodic in x and y directions, the adjacent metal strip can also be seen.

D. Impact of gap length (*g*)

Similarly, the length of the gap does not affect the scattering characteristics as shown in Figs. 14 (a) and (b) for S_{11} and S_{21}, respectively. The reason of this finding lies in the fact that there is no surface current circulation in the interior part of the metallic structure. Therefore, the existence of the gap does not affect the resonance frequency. In addition, no resonance condition is obtained for the S_{21}.

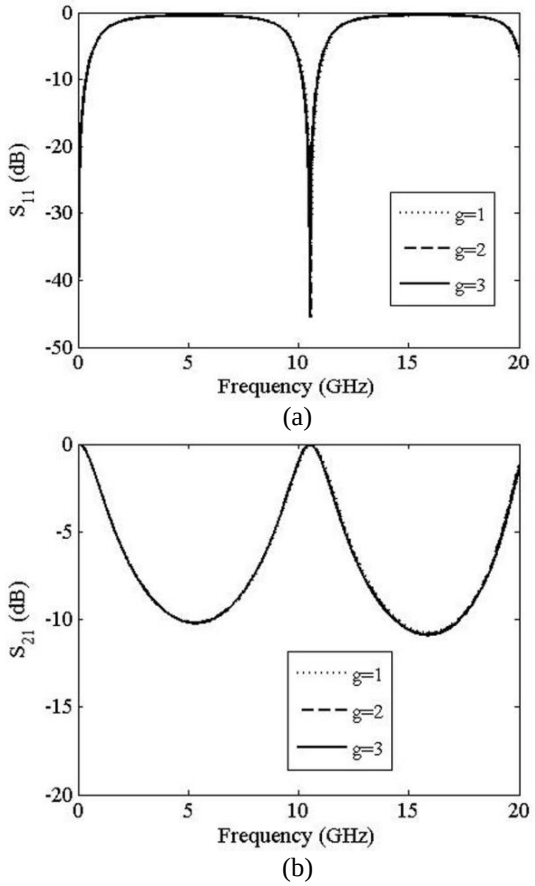

Fig. 14. Effect of gap length of a magnetically excited structure to: (a) S_{11} and (b) S_{21}. (a=10 mm, x=1 mm, g=1 mm, c=1 mm, h=1 mm, h_c=0.035 mm, and ε_r=2.2).

As shown in the corresponding results of the magnetically excited metasurface structure tunability could not be achieved since the structure parameters change the scattering characteristics negligibly or not at all.

Retrieval analysis is also conducted for the metasurface structure with magnetic excitation. Since no transmission resonance is observed for this structure, the proposed structure did not achieve to have negative region either in permittivity or permeability through the Nicholson-Ross-Weir (NRW) algorithm based on Kramers-Kronig relationship.

V. CONCLUSION

In this study, a window-like shaped novel tunable metasurface is proposed in order to be used for X and K_u band applications. The proposed structure is achieved to have dual-frequency resonance when a gap is inserted on the conductor side of the metamaterial and for each resonance frequency a single epsilon-negative region is obtained for the electrically excited structure. The structure is also evaluated under magnetic excitation conditions. However, it is observed that tunability could not be achieved; besides no single negative region is obtained for this case.

ACKNOWLEDGEMENT

We gratefully acknowledge the financial support by Scientific Research Projects of Ankara University (BAP) under Grant No. 13B4343015 and 16B0443005.

F. B. also acknowledges "The Scientific and Technological Research Council of Turkey (Tubitak)" through BIDEB-2219 Postdoctoral Research Fellowship.

REFERENCES

[1] V. G. Veselago, "The electrodynamics of substances with simultaneously negative values of ε and μ," *Soviet Physics Uspekhi*, vol. 10, no. 4, pp. 509-514, 1968.

[2] J. B. Pendry, A. J. Holden, W. J. Stewart, and I. Youngs, "Extremely low frequency plasmons in metallic mesostructures," *Phys. Rev. Lett.*, vol. 76, no. 25, pp. 4773-4776, 1996.

[3] J. B. Pendry, A. J. Holden, D. J. Robbins, and W. J. Steward, "Low frequency plasmons in thin-wire structures," *J. Phys.: Condens. Matter*, vol. 10, pp. 4785-4809, 1998.

[4] J. B. Pendry, A. J. Holden, D. J. Robbins, and W. J. Stewart, "Magnetism from conductors and enhanced nonlinear phenomena," *IEEE Trans. Microw. Theory Techn.*, vol. 47, no. 11, pp. 2075-2084, 1999.

[5] D. R. Smith, W. J. Padilla, D. C. Vier, S. C. Nemat-Nasser, and S. Schultz, "Composite medium with simultaneously negative permeability and permittivity," *Phys. Rev. Lett.*, vol. 84, no. 18, pp. 4184-4187, 2000

[6] R. Shelby, D. R Smith, and S. Schultz, "Experimental verification of a negative index of refraction," *Science*, vol. 292, no. 5514, pp. 77-79, 2001.

[7] R. Marqués, F. Mesa, J. Martel, and F. Medina, "Comparative analysis of edge- and broadside-coupled split ring resonators for metamaterial design-Theory and experiments," *IEEE Transac. Antennas Propag*., vol. 51, no. 10, pp. 2572-2581, 2003.

[8] F. Falcone, T. Lopetegi, J. D. Baena, R. Marqués, F. Martin, and M. Sorolla, "Effective negative-

epsilon stopband microstrip lines based on complementary split ring resonators," *IEEE Microw. Wireless Compon. Lett.*, vol. 14, no. 6, pp. 280-282, 2004.

[9] J. D. Baena, R. Marqués, F. Medina, and J. Martel, "Artificial magnetic metamaterial design by using spiral resonators," *Phys. Rev. B*, vol. 69, pp. 014402-1-5, 2004.

[10] D. Schurig, J. J. Mock, and D. R. Smith, "Electric-field-coupled resonators for negative permittivity metamaterials," *Appl. Phys. Lett.*, vol. 88, pp. 041109, 2006.

[11] E. Çelenk, E. Unal, D. Kapusuz, and C. Sabah, "Microstrip patch antenna covered with left handed metamaterial," *ACES Journal*, vol. 28, no. 10, pp. 999-1004, 2013.

[12] A. Jafargholi and M. Kamyab, "Dipole antenna miniaturization using single-cell metamaterial," *ACES Journal*, vol. 27, no. 3, pp. 261-270, 2012.

[13] S. Lim, C. Caloz, and T. Itoh, "Metamaterial based electronically controlled transmission-like structure as a novel-leaky wave antenna with tunable radiation angle and beamwidth," *IEEE Transac. Microw. Theory Techn.*, vol. 53, no. 1, pp. 161-173, 2005.

[14] K. L. Sheeja, P. K. Sahu, S. K. Behera, and N. Dakhli, "Compact tri-band metamaterial antenna for wireless applications," *ACES Journal*, vol. 27, no. 11, pp. 947-955, 2012.

[15] M. T. Islam, M. R. I. Faruque, and N. Bisran, "Reduction of specific absorption rate (SAR) in human head with ferrite material and metamaterial," *PIER C*, vol. 9, pp. 47-58, 2009.

[16] M. R. I. Faruque, M. T. Islam, and N. Misran, "Evaluation of EM absorption in human head with metamaterial attachment," *ACES Journal*, vol. 25, no. 12, pp. 1097-1107, 2010.

[17] Z. Szabo, G.-H. Park, R. Hedge, and E.-P. Li, "A unique extraction of metamaterial parameters based on Kramers-Kronig relationship," *IEEE Trans. Microw. Theory and Techn.*, vol. 58, no. 10, pp. 2646-2653, 2010.

Sultan Can received her B.Sc. degree in Electrical-Electronics Engineering from the Atilim University in 2008. She received her M.Sc. Degree from the same university in 2011. She is currently with the Dept. of Electrical-Electronics Engineering in Ankara University since 2013, where she is a Research Assistant and a Ph.D. Candidate. Her research interests include electromagnetism, metamaterials and antennas.

Emrullah Karakaya obtained his B.Sc. degree in Department of Engineering Physics in Ankara University, graduating in 2015. He is currently pursuing his master degree at the same department. His research interests include the analysis of frequency selective surfaces and metamaterials.

Fulya Bagci obtained her first degree in Engineering Physics from Ankara University, graduating in 2005. She received her M.Sc. and Ph.D. degrees from the same department in 2008 and 2013, respectively. Bagci is a Research Assistant in the Department of Engineering Physics, Ankara University since 2005. She has conducted postdoctoral researches at the Microwave Group in University of Sevilla (Spain), during 01.03.2015-01.03.2016. Her research interests include the analysis of frequency selective surfaces and metamaterials for photonic and microwave device applications.

A. Egemen Yilmaz received his B.Sc. degrees in Electrical-Electronics Engineering and Mathematics from the Middle East Technical University in 1997. He received his M.Sc. and Ph.D. degrees in Electrical-Electronics Engineering from the same university in 2000 and 2007, respectively. He is currently with the Dept. of Electrical-Electronics Engineering in Ankara University, where he is an Associated Professor. His research interests include computational electromagnetics, nature-inspired optimization algorithms, knowledge-based systems; more generally software development processes and methodologies.

Baris Akaoglu received his B.Sc. degree in Physics from the Middle East Technical University in 1996. He received his M.Sc. and Ph.D. degrees in Physics from the same university in 1998 and 2004, respectively. He is currently with Department of Engineering Physics in Ankara University, where he is a Professor. He did experimental research on semiconductors. His current research interests include photonic crystals and metamaterials.